

Effect of Foundation Width on Subgrade Reaction Modulus

Takashi Nagao

Research Center for Urban Safety and Security
Kobe University
Kobe City, Japan
nagao@people.kobe-u.ac.jp

Abstract—Structures are subjected to vertical and horizontal loads. Vertical subgrade reaction acts on the foundation bottom surface, and in the case of an embedded structure, horizontal subgrade reaction acts on the embedded part. The subgrade reaction is obtained by multiplying the displacement of the foundation by the Subgrade Reaction Modulus (SRM). In practice, SRM is calculated using an equation that incorporates the negative power relationship of the Foundation Width (FW). If the structure is evaluated to be poorly seismic resistant, it is necessary to widen FW. However, when the FW is widened, the design value of SRM decreases. In this case, it is not possible to expect an increase in the subgrade reaction proportional to the increase of FW. Therefore, when the inertia force is very high, the FW has to be very wide. However, underestimating SRM can lead to structural overdesign. In this study, the relationship between SRM and FW, for a structure in which vertical and horizontal load act simultaneously, was analyzed. Compared with the design practice assumptions, the horizontal SRM was found to be highly dependent on FW while the vertical SRM was shown to be less dependent on FW.

Keywords—subgrade reaction modulus; soil stiffness; foundation width

I. INTRODUCTION

During an earthquake, structures undergo vertical loads, such as dead weight, and horizontal loads, such as the inertia force. In response to these loads, the vertical subgrade reaction acts on the bottom surface of the structure foundation. For structures with embedded foundations, the horizontal subgrade reaction acts as a resistance force on the embedded foundation. The subgrade reaction is obtained by multiplying the Subgrade Reaction Modulus (SRM) by the displacement of the foundation. Parameters that affect SRM include ground stiffness and Foundation Width (FW). It has been pointed out that SRM increases with increasing ground stiffness and decreases with increasing FW [1-6]. For this reason, SRM calculation equations comprising ground stiffness and FW have been incorporated into various design specifications [7]. Although various equations have been proposed for the evaluation of SRM, the degree of dependence of SRM on FW varies in different studies. When an external force such as the seismic load is evaluated to be large, or when a large lateral spreading pressure is expected to act during an earthquake [8],

FW needs to be widened to enhance seismic resistance. However, since the SRM calculation equation with negative power relationship of FW is used in design practice, widening FW lowers SRM. As a result, an increase in the subgrade reaction proportional to the increase in FW cannot be expected. Therefore, if the seismic load is very large, FW should be very wide. Conversely, an experimental study on the seismic resistance of piers with various FWs has shown that the piers with wider FWs are extremely seismic resistant due to the increase in vertical subgrade reaction [9]. The results have shown that the calculation equation of the design practice could underestimate SRM for wide FW conditions. Therefore, applying the SRM calculation equation of current design specifications can lead to structural overdesign under very high seismic loads. In this study, the relationship between SRM and FW was analyzed for structures under simultaneous vertical and horizontal loads.

II. CONVENTIONAL EVALUATION METHOD OF SRM

Numerous studies have been performed to evaluate SRM. The following are typical SRM calculation equations:

$$k_s = \frac{0.95}{B} \left(\frac{E_s}{1-\nu_s^2} \right) \left(\frac{E_s B^4}{EI} \right)^{0.108} \quad (1)$$

$$k_s = k_{0.3} \left(\frac{B+0.3}{2B} \right)^2 \quad (2)$$

$$k_s = \frac{0.65}{B} \left(\frac{E_s}{1-\nu_s^2} \right)^{1/2} \sqrt{\frac{E_s B^4}{EI}} \quad (3)$$

$$k_s = \frac{1}{0.3} \alpha E_s \left(\frac{B}{0.3} \right)^{-3/4} \quad (4)$$

where k_s is the SRM, $k_{0.3}$ is the SRM obtained by a plate loading test with a width of 0.3m, B is the FW, E_s and ν_s are Young's modulus and Poisson's ratio of the ground respectively, and EI is the flexural rigidity of the foundation. Equations (1)–(3) have been proposed in [1–3] respectively. Equation (4) is an equation of the Japanese Specifications for Highway Bridges (JSHB) [7]. The JSHB equation is based on the results of field horizontal loading experiments [4] in which the dependence of horizontal SRM on the width of a loading

Corresponding author: Takashi Nagao

plate was discovered. In (4), coefficient α is specified as 2 (for example) when E_s is evaluated by N -values from the standard penetration tests to obtain the SRM values during an earthquake. All these equations show that SRM decreases with increasing FW.

Figure 1 shows how the SRM varies over the FW range of 4–10m. The values of (1) to (4) are shown in red, blue, green, and black lines respectively. The SRM results from (2) (blue line) are slightly affected by FW, whereas the other results are significantly influenced by FW. The SRM results of (4) show the largest decrease with increasing FW.

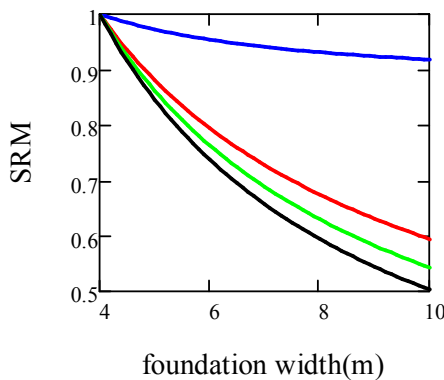


Fig. 1. Comparison of SRM results.

The characteristics of ground stress propagation are briefly explained to understand the reason why the SRM calculation equation has been proposed in accordance with FW. When a distributed load is applied on the ground from the structure, the stress propagates in the ground. The propagated stresses caused by loads at different locations on the ground surface are superimposed in the ground. The values of stresses superimposed in the ground increase with increasing FW. Therefore, even if the stresses on the ground surface are the same, the amount of ground deformation increases with increasing FW. Since SRM is a value obtained by dividing a ground surface stress by the amount of displacement, it becomes smaller when the FW is wider. Therefore, the existing equations are dependent on FW, and SRM decreases with increasing FW. However, the degree of the dependency of SRM on FW may be different for horizontal and vertical SRMs. Since the ground normally has a constant stiffness (Young’s modulus) in the horizontal direction, the above idea may be valid. However, in the vertical direction, Young’s modulus generally increases with increasing depth. If the Young’s modulus is large, the deformation becomes small even if the same stress is applied. Therefore, even under the same stress increments, the amount of ground deformation decreases with increasing depth. Since the amount of deformation at the ground surface is calculated as the sum of the amounts of deformation in the ground, the degree of decrease in vertical SRM with respect to the increments of ground stress may be insignificant. Moreover, for structures with embedment, the foundation is usually embedded in soil layers with very high Young’s modulus. For this reason, vertical SRM is less dependent on FW than horizontal SRM.

III. EVALUATION OF VERTICAL SRM

Boussinesq’s equation is known for evaluating the stress in the ground when a concentrated load acts on a semi-infinite elastic three-dimensional ground surface. The equation for calculating the stress in the ground under distributed load acting on two-dimensional elastic ground is obtained by integrating Boussinesq’s equation [10]. As shown in Figure 2, the vertical ground stress (σ_z) at point P under a uniformly distributed load is obtained by:

$$\sigma_z = \frac{q}{\pi} \{ \theta_1 + \theta_2 + \sin(\theta_1 + \theta_2) \cos(-\theta_1 + \theta_2) \} \quad (5)$$

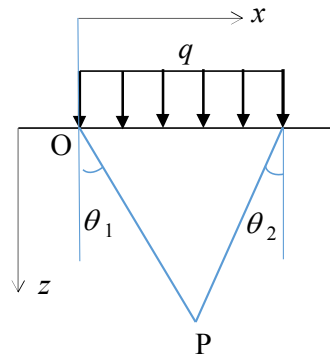


Fig. 2. Uniformly distributed load.

When a structure undergoes vertical and horizontal loads simultaneously, (i) a horizontally distributed load and (ii) a vertically trapezoidal (or triangular) distributed load act simultaneously on the ground surface. When the horizontal load is relatively small compared to the vertical load, the vertically distributed load on the ground surface shows a trapezoidal distribution, and when the horizontal load is large, it shows a triangular distribution. Since a trapezoidal distributed load can be expressed as a combination of a uniformly distributed load and a triangular distributed load, the equation for calculating the ground stress under a triangular distributed load can be explained. As shown in Figure 3, when a triangular distributed load with intensity q at the origin is applied, the vertical stress at point P is calculated as [11]:

$$\sigma_z = \frac{q}{\pi} \left\{ (\theta_1 + \theta_2) \frac{\sin(\theta_2) \cos(\theta_1)}{\sin(\theta_1 + \theta_2)} + \sin(\theta_1) \cos(\theta_1) \right\} \quad (6)$$

Furthermore, as shown in Figure 4, when a horizontally distributed load is applied, the vertical stress at point P is calculated as follows [11]:

$$\sigma_z = \frac{q}{\pi} \sin(\theta_1 + \theta_2) \sin(\theta_2 - \theta_1) \quad (7)$$

Regarding the ground condition, it was considered to be composed of two layers with a thickness of 10m. The saturated unit weight of soil in each layer was 20kN/m³, Poisson’s ratio (ν) was 0.33, and the water table was on the ground surface. Two ground conditions were assumed: soft ground condition (Case 1) and hard ground condition (Case 2). N_{65} was set for each layer to evaluate Young’s modulus of the ground under

each condition. Here, N_{65} represents the N -value when the effective overburden pressure (σ_v') is 65kPa. In Case 1, N_{65} was 10 in the middle of the upper layer and 20 in the middle of the lower layer. In Case 2, N_{65} was 30 in the middle of the upper layer and 45 in the middle of the lower layer. The relationship between N_{65} and N -value under σ_v' is [12]:

$$N_{65} = \frac{N - 0.019(\sigma_v' - 65)}{0.0041(\sigma_v' - 65) + 1.0} \quad (8)$$

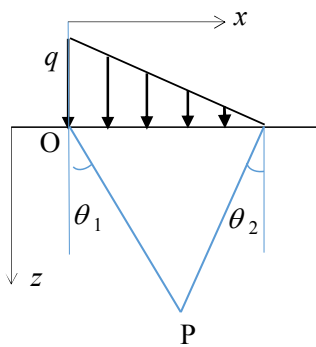


Fig. 3. Triangular distributed load.

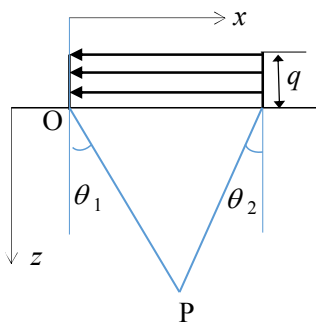


Fig. 4. Horizontally distributed load.

To calculate Young's modulus of the ground, the shear modulus G (kPa) was obtained from the N -value using (9) [13]. Young's modulus E was calculated with (10):

$$G = 14400N^{0.88} \quad (9)$$

$$E = 2(1 + \nu)G \quad (10)$$

Young's modulus of the soil was treated as the average effective confining stress dependent as follows:

$$E = \left(\frac{\sigma_m'}{\sigma_{ma}'} \right)^{mg} E_a \quad (11)$$

where E is the Young's modulus, E_a is the reference Young's modulus, σ_m' is the average effective confining stress, σ_{ma}' is the reference average effective confining stress, and mg is the exponent that represents the average effective confining stress dependency of the modulus (= 0.5 in this study, based on [14]). It is assumed that there is a bedrock with a very large Young's

modulus below the lower layer in which the deformation can be ignored.

As shown in Figure 5, a case with a structure with 20kN/m³ unit weight and 8m height installed on the ground surface was considered. FW was set to 4, 6, 8, and 10m. The structure was assumed to receive a seismic load with a seismic coefficient of 0.3 at a height of 4m from the ground surface, which was the gravity center of the structure. The seismic coefficient is the ratio of seismic load to dead weight. The vertical load distribution on the ground surface became a trapezoidal distribution under the current study condition. A rotational resistance moment was generated due to the distributed load to resist the moment load caused by the seismic load. The intensity of the vertically distributed load on the ground surface was calculated from the moment balance equation. For comparison, the calculation was also performed under the condition that there was no horizontal load and only a uniformly distributed vertical load was applied on the ground surface.

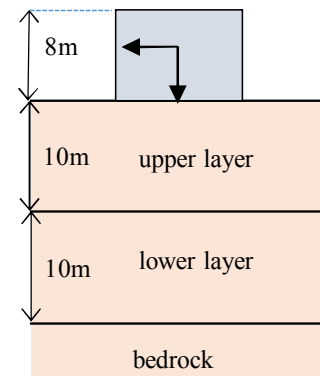


Fig. 5. Study condition.

Figures 6 and 7 illustrate the depth distributions of σ_z for FWs of 4m and 10m respectively. The red, blue, and green lines are the results at $x = B/8, B/4,$ and $B/2$ in Figures 2–4, respectively, where B is the FW. When only uniformly distributed vertical loads were applied, the stresses on the ground surface were the same regardless of the position in the horizontal direction. The ground stresses were smaller near the foundation edge and larger near the foundation center due to the superposition of ground stresses. The ground stresses decreased rapidly with increasing depth and became almost the same regardless of the horizontal position below -10m for FW equal to 4m and below -20m for FW equal to 10m. The narrower the FW, the smaller the difference in ground stress due to the difference in horizontal positions, because the narrower the FW, the smaller the effect of stress superposition. When a vertically trapezoidal distributed load was applied, the stress on the ground surface changed significantly depending on the distance from the foundation edge, but the stress decreased sharply as the depth increased. The stresses did not differ depending on the horizontal position at -5m depth for FW 4m and at -10m for FW 10m.

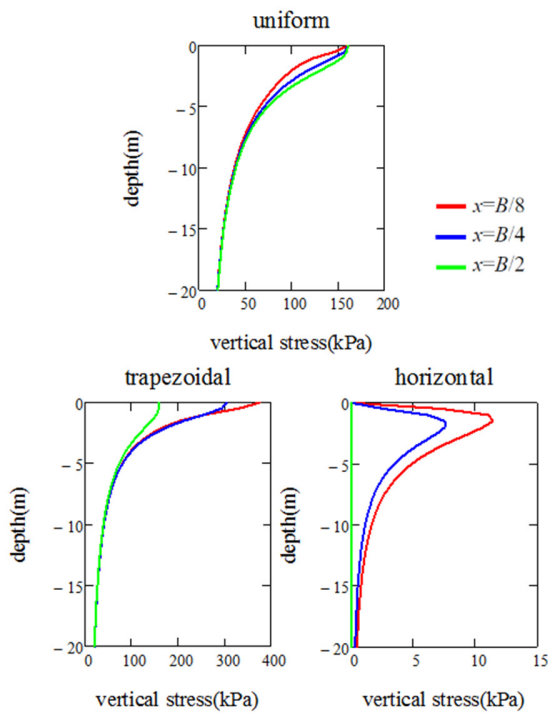


Fig. 6. Vertical stress depth distribution (4m width).

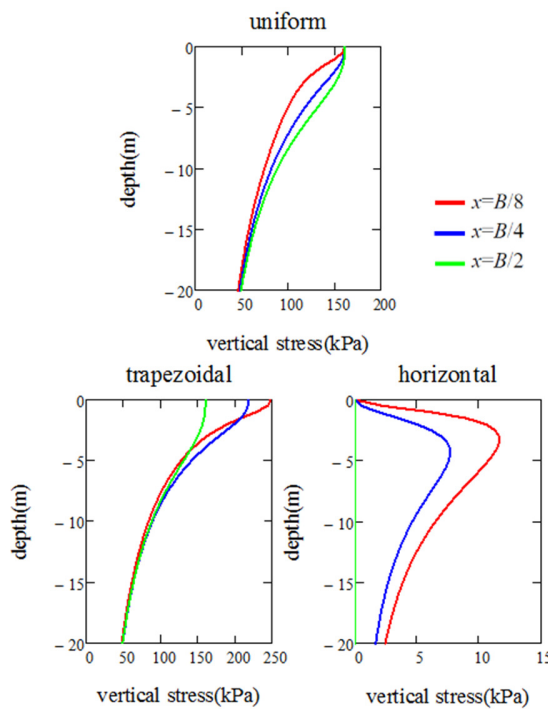


Fig. 7. Vertical stress depth distribution (10m width).

The stresses due to the horizontally distributed loads on the ground surface became very small ranging from zero on the ground surface to maximum at depths of -2 to -3 m. The stress was zero at the foundation center regardless of the depth, with positive and negative reversal around the foundation center. Figures 8 and 9 compare the depth distributions of stresses at

positions from the foundation edge of $B/4$ and $B/2$ respectively, under the condition that vertically trapezoidal and horizontally distributed loads were applied simultaneously. The red, blue, green, and black lines are the results for $B = 4, 6, 8,$ and 10 m, respectively. When the FW was narrow, the stress at the $B/4$ position became large on the ground surface. However, the stress sharply decreased with increasing depth, and when the FW became narrower, the ground stress below -2 m became smaller. At the foundation center, the stresses on the ground surface were the same, and with increasing depth, the stresses decreased sharply. The stresses were always smaller for narrower FWs.

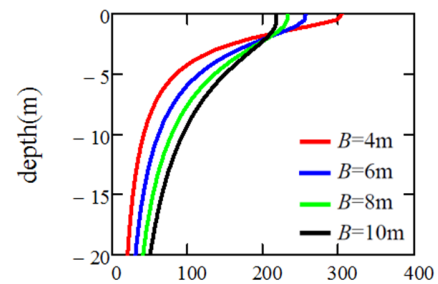


Fig. 8. Vertical stress depth distribution (at $B/4$).

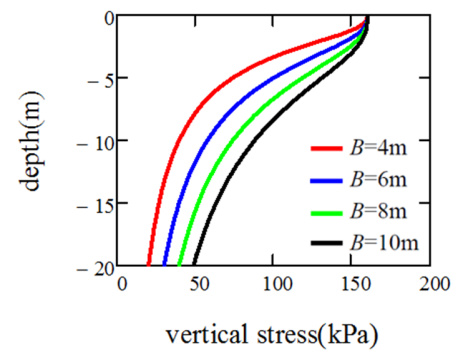


Fig. 9. Vertical stress depth distribution (at $B/2$).

Figure 10 exemplifies the foundation settlement distribution under uniformly distributed loads for FW equal to 4m in Case 1. Since the theoretical equations were adopted in this study, the boundary conditions at the foundation edge were not sufficiently considered. Although only uniform vertical loads were applied to the ground surface, the foundation settlement distribution was not uniform. Therefore, the SRM was calculated by excluding the results at the foundation edge. Figures 11 and 12 demonstrate the changes in SRM with changing FW. The red line shows the results in the case of only uniformly distributed loadings, and the blue line represents the results of simultaneous vertically trapezoidal and horizontally distributed loadings. These results were not significantly different. The results obtained from the JSHB equation (shown by the green line) show changes in SRM with changing FW under the condition where the SRM results from the JSHB equation and the theoretical SRM were the same when vertically trapezoidal and horizontally distributed loads were applied simultaneously to a FW of 4m. As can be seen in the

Figures, the impact of FW was present, and SRM decreased with increasing FW, but the degree of SRM decrease with increasing FW was very small for every ground condition. The JSHB equation overestimated the effect of FW, and when the FW was extended, SRM was significantly underestimated. This was because the amount of settlement was small at greater depths due to the ground stiffness. Furthermore, the ground stress increased with increasing FW, but the amount of settlement did not increase significantly when the FW increased. As mentioned above, the JSHB equation is based on the horizontal loading test results and is not suitable for evaluating the vertical SRM.

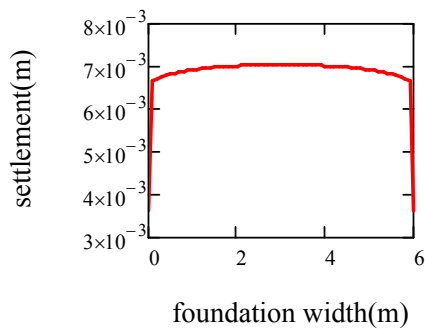


Fig. 10. Settlement distribution (FW 4m).

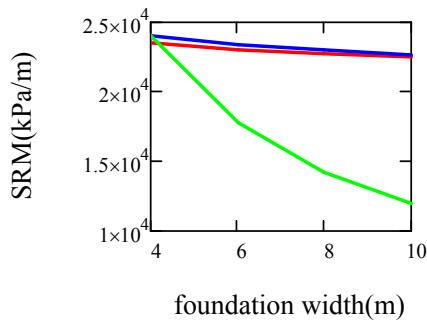


Fig. 11. Vertical SRMs (Case 1).

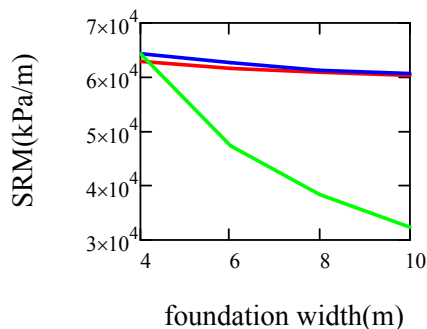


Fig. 12. Vertical SRMs (Case 2).

IV. EVALUATION OF HORIZONTAL SRM

The ground conditions are similar to the previous section, and the effects of FW on the horizontal SRM with embedded

structures are discussed in the current section. Figure 13 shows the study conditions. It was assumed that the structures with a width of 2m and different dimensions in depth were embedded to the lower end of the upper soil layer. Unit weight, seismic coefficient, and location of seismic loads in the structure are the same as in the previous chapter. The SRM evaluation position is in the middle of the upper layer. Equation (5) can be applied to the calculation of the horizontal ground stress caused by seismic load, since a uniformly distributed horizontal load is assumed in the depth direction. When a structure with high flexural rigidity rotates around the bottom due to the action of seismic load, it is linearly displaced from the bottom of the structure toward the ground surface, resulting in linear ground deformation and ground stress. The ground stress at the SRM evaluation position was calculated under this assumption.

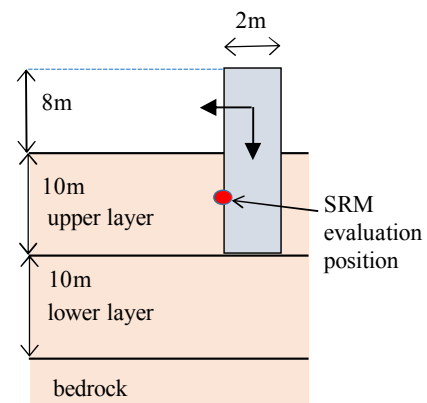


Fig. 13. Study condition.

Figure 14 illustrates the changes of horizontal ground stress distribution due to the changes in FW, plotted against the horizontal distance from the SRM evaluation position. The horizontal ground stress distributions were similar to the stress distribution pattern shown in Figure 9. However, since Young's modulus is constant in the horizontal direction, a large difference occurred in the amount of deformation due to differences in ground stress at points away from the foundation. As a result, when the FW were different, the SRM values were significantly different.

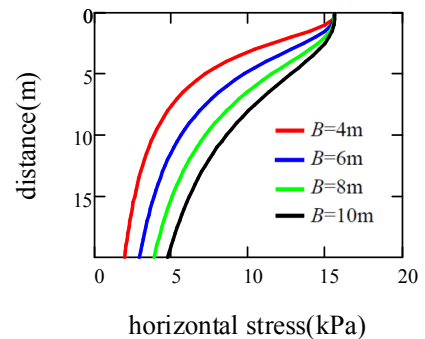


Fig. 14. Horizontal ground stress distribution.

Figures 15 and 16 demonstrate the changes in SRM with changes in FW (red line) with an obvious dependence on FW. The green lines in the Figures represent the SRM results obtained from the JSHB equation. They show changes in SRM in response to the changes in FW when the SRM results obtained from the JSHB and the theoretical equations were the same at the FW of 4m. The JSHB equation overestimates the FW dependence but to a lesser extent compared to the vertical SRM results. Therefore, the JSHB equation has some applicability in evaluating horizontal SRM.

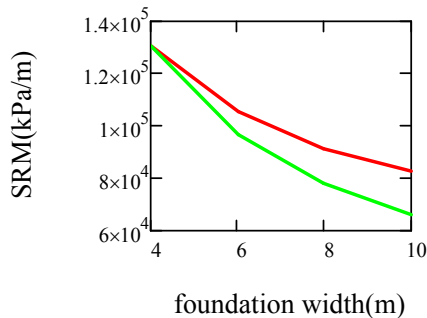


Fig. 15. Horizontal SRMs (Case 1).

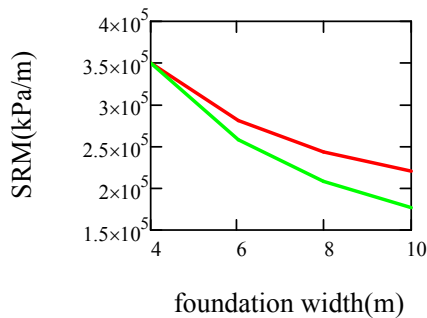


Fig. 16. Horizontal SRMs (Case 2).

V. CONCLUSIONS

This study discussed the applicability of the SRM design equations by comparing the analytical results with the ones produced by the JSHB equation at various FWs. For horizontal SRM, the effect of FW was relatively high, and the JSHB equation was found to be applicable to some extent. However, in the case of vertical SRM, since Young's modulus of the ground depends on depth, the effect of FW was found to be weak, and for wide FW, the JSHB equation underestimated SRM significantly. The relationship between stress and deformation of the soil is linear and the SRM is the ratio of stress to deformation, therefore the effect of FW on SRM found in this study applies regardless of the ground and loading conditions. When the seismic load is expected to be large, the FW needs to be widened. However, underestimating vertical SRM may result in structural overdesign. Therefore, a successful design practice requires proper evaluation of vertical SRM.

ACKNOWLEDGMENT

This research was supported by JSPS KAKENHI, Grant Number JP18K04324.

REFERENCES

- [1] M. A. Biot, "Bending of an Infinite Beam on an Elastic Foundation," *Journal of Applied Mathematics and Mechanics*, no. 203, pp. A1-A7, Mar. 1937.
- [2] K. Terzaghi, "Evaluation of Coefficients of Subgrade Reaction," *Géotechnique*, vol. 5, no. 4, pp. 297-326, Dec. 1955, doi: 10.1680/geot.1955.5.4.297.
- [3] A. B. Vesic, "Beams on Elastic Subgrade and the Winkler's Hypothesis," in *Proceedings of 5th International Conference of Soil Mechanics*, 1963, pp. 845-850.
- [4] T. Yoshinaka, "Subgrade reaction coefficient and its correction based on the loading width," PWRI Report 299, 1967.
- [5] R. Ziaie-Moayed and M. Janbaz, "Effective Parameters on Modulus of Subgrade Reaction in Clayey Soils," *Journal of Applied Sciences*, vol. 9, pp. 4006-4012, doi: 10.3923/jas.2009.4006.4012.
- [6] J. Lee and S. Jeong, "Experimental Study of Estimating the Subgrade Reaction Modulus on Jointed Rock Foundations," *Rock Mechanics and Rock Engineering*, vol. 49, no. 6, pp. 2055-2064, Jun. 2016, doi: 10.1007/s00603-015-0905-9.
- [7] *Specifications for Highway Bridges, Part IV, Substructures*. Japan Road Association, 2016.
- [8] T. Nagao and D. Shibata, "Experimental Study of the Lateral Spreading Pressure Acting on a Pile Foundation During Earthquakes," *Engineering, Technology & Applied Science Research*, vol. 9, no. 6, pp. 5021-5028, Dec. 2019.
- [9] T. Nagao, "An Experimental Study on the Way Bottom Widening of Pier Foundations Affects Seismic Resistance," *Engineering, Technology & Applied Science Research*, vol. 10, no. 3, pp. 5713-5718, Jun. 2020.
- [10] J. H. Michell, "On the Direct Determination of Stress in an Elastic Solid, with application to the Theory of Plates," *Proceedings of the London Mathematical Society*, vol. s1-31, no. 1, pp. 100-124, 1899, doi: 10.1112/plms/s1-31.1.100.
- [11] T. Kimura, "Analytical investigation on mechanical behaviors of two-layer systems," *Proceedings of the Japan Society of Civil Engineers*, vol. 1969, no. 162, pp. 31-48, Feb. 1969.
- [12] *Technical standards and commentaries for port and harbour facilities in Japan*. Overseas Coastal Area Development Institute of Japan, 2009.
- [13] T. Imai and K. Tonouchi, "Correlation of N-value with S-wave velocity and shear modulus," in *Proceedings of the 2nd ESPT*, Rotterdam, Netherlands, 1982, pp. 67-72.
- [14] I. Suetomi and N. Yoshida, "Nonlinear Behavior of Surface Deposit during the 1995 Hyogoken-Nambu Earthquake," *Soils and Foundations*, vol. 38, Supplement, pp. 11-22, Sep. 1998, doi: 10.3208/sandf.38.Special_11.